

Microstructure of lateral epitaxial overgrown InAs on (100) GaAs substrates

G. Suryanarayanan

Materials Science Program, University of Wisconsin, Madison, Wisconsin 53706

Anish A. Khandekar and Thomas F. Kuech

Department of Chemical Engineering, University of Wisconsin, Madison, Wisconsin 53706

Susan E. Babcock^{a)}

Department of Materials Science and Engineering and Materials Science Program, University of Wisconsin, Madison, Wisconsin 53706

(Received 6 June 2003; accepted 15 July 2003)

Substantial defect reduction was achieved in InAs/GaAs by lateral epitaxial overgrowth in which InAs was grown on mask-patterned (100) GaAs with stripe-shaped windows of various widths by metalorganic chemical vapor deposition. The InAs growth morphology, crystal quality, and microstructure were evaluated using double-crystal x-ray rocking curves and scanning and transmission electron microscopy. The microstructure of the InAs grown on mask-free control samples was comprised of micron-scale misoriented grains and dislocations at a density of 10^{11} cm^{-2} . As the width of the mask openings decreased to $0.8 \mu\text{m}$, the rocking curves narrowed, grain boundaries disappeared and the dislocation density decreased to $<10^7 \text{ cm}^{-2}$. The distribution of the remaining defects suggests substantial changes in microstructural development when the window width is $\leq 1 \mu\text{m}$. © 2003 American Institute of Physics. [DOI: 10.1063/1.1609231]

InAs and GaSb constitute a near-lattice-matched epitaxial system that has found device applications in high-speed electronics,¹ thermophotovoltaics,² and optical emitters/detectors.³ The performance of many of these devices is enhanced when the substrate is insulating. High-crystal-quality InAs and GaSb substrates can be produced by conventional bulk growth techniques. However, neither material is readily grown with high resistivity or semi-insulating character, hence, semi-insulating GaAs typically is employed as the substrate for InAs and GaSb-based electronics.⁴ The consequent large lattice mismatch of $\sim 7\%$ between the device materials and GaAs substrate often leads to high defect densities and complex defect microstructures within the device layers. Some defect reduction⁵ and the demonstration of a variety of arsenide and antimonide-based device structures^{6,7} have been achieved via addition of a buffer layer. In other materials systems, most notably GaN on SiC and sapphire, lateral epitaxial overgrowth (LEO) has effected substantial defect reduction.^{8,9} This letter reports on the crystal quality and microstructure of InAs grown directly on GaAs using a LEO approach, illustrated in Fig. 1(a). A critical importance of the window dimension is revealed for this system. Substantial defect reduction and, more significantly, alterations in the epitaxy and defect microstructure are observed when the window opening has submicron dimensions.

The LEO substrates consisted of 0° -miscut (100) GaAs wafers onto which $\sim 120 \text{ nm}$ of SiO_2 was deposited by low-pressure chemical vapor deposition. Stripe-shaped windows of width $0.8, 2,$ and $5 \mu\text{m}$ were etched into the SiO_2 at $10 \mu\text{m}$ pitch using standard photolithographic and etching techniques. The long axis of the stripes was oriented along the

GaAs $[01\bar{1}]$ to maximize the lateral growth rate of the InAs.¹⁰ InAs epilayers were grown by metalorganic chemical vapor deposition in a horizontal quartz reactor at 700°C and 78 Torr . The substrates were annealed in arsine for 10 min at 700°C to desorb the surface oxides prior to growth. Trimethylindium and arsine were used as precursors in a Pd-diffused H_2 carrier gas at a V/III ratio of 80 .¹¹ Each growth run included both LEO and unpatterned (100) GaAs (i.e., control, or, equivalently, infinite-window width) substrates. InAs was grown directly on the GaAs surface; no buffer layers were introduced. InAs nucleated on the exposed GaAs in all cases; no evidence of InAs nucleation on the SiO_2 mask was found for any of the substrate geometries examined here. Scanning electron microscopy (SEM), x-ray dif-

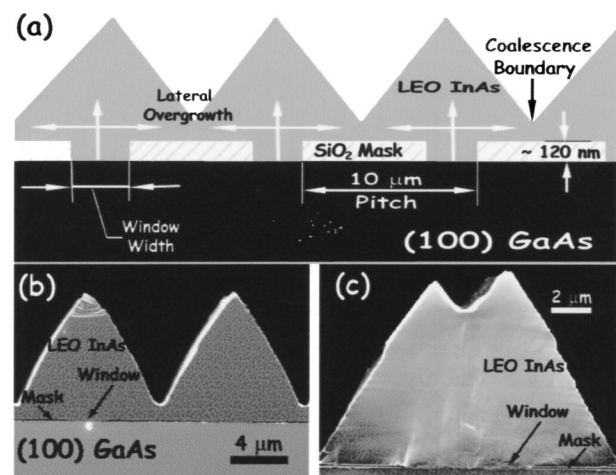


FIG. 1. (a) Schematic of the LEO process. (b),(c) SEM micrographs of cross-sectional fracture surfaces of LEO InAs grown for 2.5 h with 2 and $5 \mu\text{m}$ windows, respectively.

^{a)}Electronic mail: babcock@engr.wisc.edu

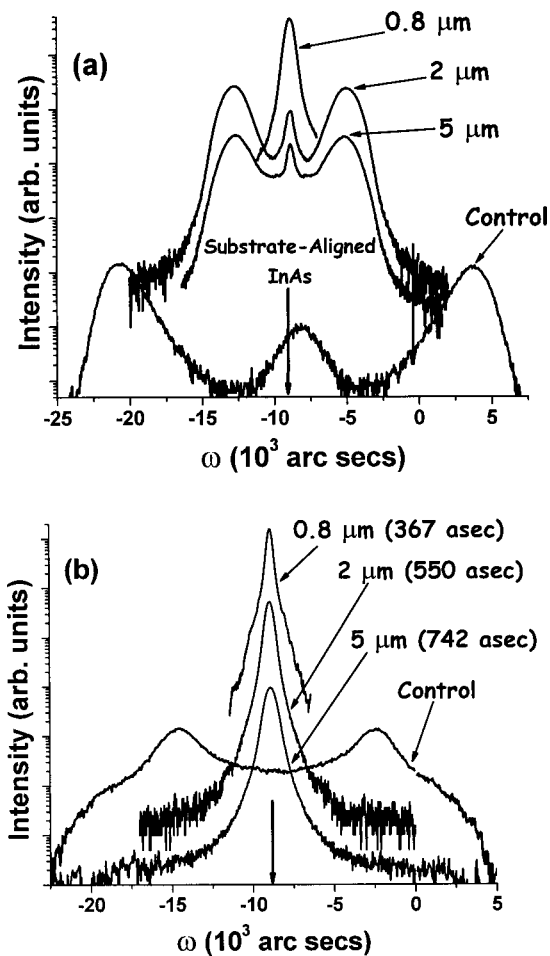


FIG. 2. (400) Rocking curves for LEO and control InAs: (a) perpendicular and (b) parallel to $[01\bar{1}]$ long axis of the stripes. In (b) the FWHM are given in parentheses. Curves have been displaced arbitrarily along the ordinate for clarity. The arrow on the abscissa indicates the peak position of substrate-aligned InAs.

fraction, and cross-sectional transmission electron microscopy (TEM) techniques were used to characterize the growth topography, crystal quality, and internal defect microstructure. TEM specimens were prepared by tripod polishing followed by short-duration (≤ 2.5 hrs) ion milling.

Figure 1 shows cross-sectional secondary-electron SEM micrographs of as-cleaved LEO samples with 2 and 5 μm window openings. The generally triangular cross section of the “bars” of growth above the window is typical for windows oriented along GaAs $[01\bar{1}]$. The growth has proceeded to coalescence of neighboring bars, resulting in a 1–3- μm -thick continuous film of InAs. The coalescence boundary is void free. The film surface is rough on the scale of micrometers due to the inclination of the slow-growth planes. The bar sidewalls are the $\{111\}$ A slow-growth planes of InAs. As the window opening increased from 2 to 5 μm , the surface morphology above each window evolved into a double-ridge structure with the same $\{111\}$ A type sidewalls. In a parallel study multiple ridges formed above windows with yet wider openings.¹⁰

Double-crystal x-ray rocking curves were used to characterize the general crystal quality as a function of the width of the window. The rocking curves in Fig. 2 show a dependence of InAs orientation and mosaic spread on both window width and crystallographic direction. The rocking curve ge-

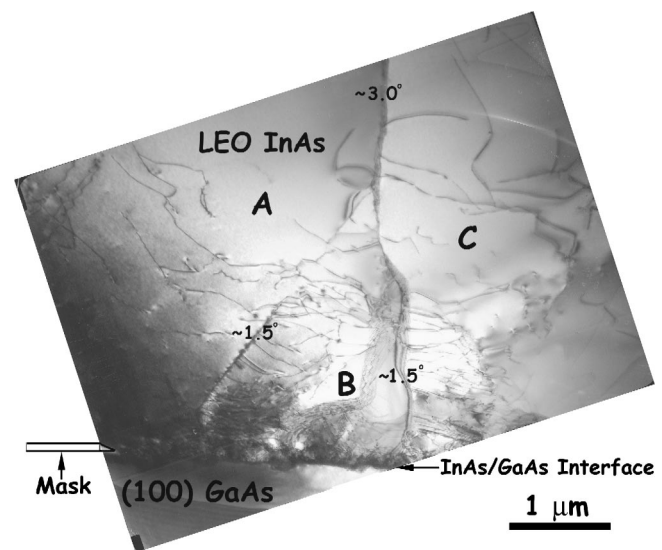


FIG. 3. (022) bright-field TEM micrograph of the window region of a LEO sample with 5 μm wide windows. The cross-sectional specimen is cut perpendicular to the long axis of the windows. Grain boundary labels are misorientation angles determined from selected area diffraction patterns.

ometry for Fig. 2(a) $[(2b)]$ probed crystal orientation and (400) mosaic spread perpendicular (parallel) to the long axis of the window. For InAs on the infinite-window-width (i.e., unpatterned) substrate, both rocking curves have multiple broad peaks separated by 5° – 7° that indicate the presence of several epitaxial orientation relationships. Some of the InAs is aligned crystallographically with the GaAs substrate, whereas some are misoriented by a few degrees. As the mask is introduced and further as the windows become narrower, the angles of misorientation in scans perpendicular to the long axis of stripes decrease until a single orientation, in registry with the (100) GaAs, is observed for the 0.8 μm wide windows [Fig. 2(a)]. Along the stripe axis, a single orientation, aligned with the GaAs substrate, was observed for all LEO samples [Fig. 2(b)]. The explanation for this counterintuitive anisotropy in the evolution from multiple to single InAs orientation with respect to the scan orientation is not yet clear. Nevertheless, it does suggest a basic change in the epitaxy and microstructure of InAs as the window opening decreases to submicron values. In addition the full width at half maximum (FWHM) of all of the peaks in both directions decreases with decreasing window width, indicating a concomitant general improvement in crystal quality.

Cross-sectional TEM of InAs films grown on substrates with infinitely, 5 μm and 0.8 μm wide windows revealed microstructures and microstructural changes that were both consistent with the x-ray rocking curves and indicative of basic changes in microstructural development with narrowing window width. Two features that dominate the microstructure of InAs grown on the infinite-window substrate are shown in Fig. 3(a) of Ref. 12. They are: (a) low-angle grain boundaries that thread the film from substrate to surface and separate grains, each of which are misoriented by $\sim 3^\circ$ relative to the substrate, and (b) sets of dislocations that appear at many locations throughout the film. The grain size near the substrate is ~ 1 μm . It coarsens to ~ 3 μm within the first few microns of growth as a result of impingement and reaction of neighboring grain boundaries. Figure 3 shows an

TABLE I. Estimated dislocation density as a function of distance from the GaAs substrate.

Distance from the InAs/GaAs interface (μm)	0.8 μm window (cm^{-2})	5 μm window (cm^{-2})	Infinite (cm^{-2})
Within 0.15	$>10^{11}$	$>10^{11}$	$>10^{11}$
0.15–3	7×10^8	8×10^9	1×10^{10}
>3	9×10^6	1×10^9	Exceeds film thickness

example of such a reaction above a 5 μm wide window in a LEO film; such reactions occur throughout the control film. The bias towards certain specific grain boundary misorientations of 2° – 3° observed, albeit with the small statistics typical of TEM, is quantitatively consistent with the peak splitting observed in the x-ray rocking curves for this sample. Presumably the dislocation networks contribute to the breadth of the individual peaks in both the infinite and 5 μm LEO samples. Estimates of the dislocation density as a function of distance from the substrate are given in Table I.

A bimodal microstructure was observed in the films grown on LEO substrates, in that the microstructure of the material above the window differed systematically from that above the mask. The microstructure above the 5 μm wide window in Fig. 3 is qualitatively the same as that observed throughout the control sample. Low-angle grain boundaries that intersect and combine as the film thickens thread the film from the substrate to surface intersecting it at the valley of the double ridge. Above every window studied (9), there exist at least two grains misoriented by a few degrees with respect to each other. In contrast, no new grains, and thus no new low-angle grain boundaries form in the overgrown material above the mask. Thus, defect reduction roughly in proportion to the mask-to-window surface area (Table I) is realized in this film, consistent with the sharpening of the x-ray rocking curve peaks. The origin of the reduction in grain boundary misorientation angle is not clear from these cross sections.

The TEM micrograph in Fig. 4 shows the basic changes

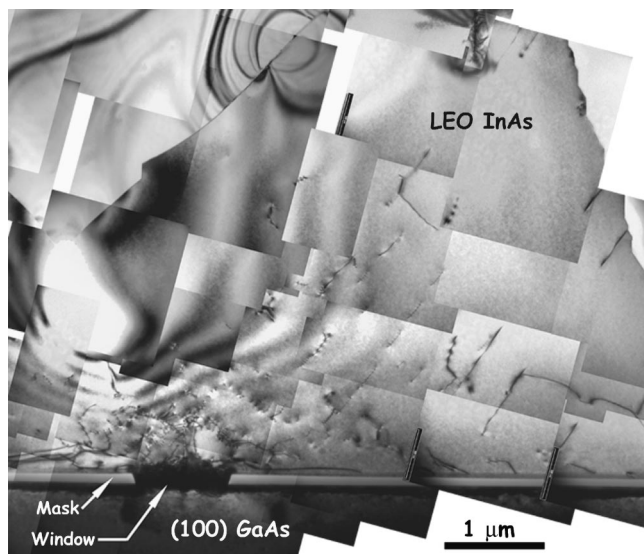


FIG. 4. (022) bright-field TEM micrograph of defect microstructure in the LEO InAs grown on 0.8 μm windows.

in the defect microstructure that occur in both the vicinity of the window and in the entire film when the window width is reduced further to 0.8 μm . First, a single low-angle grain boundary bisected almost every window of the 17 observed. In contrast to growth on the other substrates, however, the misorientation angle of each boundary above the 0.8 μm wide windows decreased with distance from the substrate until the boundary effectively terminated $\sim 0.75 \mu\text{m}$ into the film. Second, the material directly above the exposed GaAs is heavily populated with dislocations. However, these dislocations are confined to the volume just above the window and within about 0.25 μm from the GaAs surface. Elsewhere in the film the dislocation density is reduced by more than two orders of magnitude (Table I). Third, there is evidence that dislocations in the window region are induced to lie parallel to the substrate, rather than thread to the film surface. Fourth, it appears possible for the plane of intersection of two neighboring overgrowths to be defect free [see Fig. 3(b) of Ref. 12].

The general reduction in defect density, Table I, is consistent with the reduction in x-ray linewidth with decreasing window width. Similarly, the termination of the low-angle grain boundary in the first three-quarter micrometers of growth is consistent with the loss of multiple peaks in the x-ray rocking curves. The latter also suggests that the changes in microstructure are driven by factors in the growing film rather than upon nucleation.

These studies show that defect reduction is realized upon application of the LEO technique to the InAs/GaAs system. More importantly, the basic character of the microstructure changes in a way that accelerates defect reduction when the window width is less than $\sim 1 \mu\text{m}$. The origin of the defect reduction when using submicrometer window openings is not understood at present. Possibly the narrowing of the window width to dimensions where the stress fields induced by the patterned mask are of the same length scale as the mask itself drives this transition. Whether this underlying stress or some additional interaction is responsible for the change in the microstructure and defect density, it is clear that there are effects that allow for the direct manipulation of the defect structure at these dimensions.

¹C. R. Bolognesi, J. D. Werking, E. J. Caine, H. Kroemer, and E. L. Hu, IEEE Electron. Device Lett. **14**, 13 (1993).

²L. M. Fraas, G. R. Girard, J. E. Avery, B. A. Arau, V. S. Sundaram, A. G. Thompson, and J. M. Gee, J. Appl. Phys. **66**, 3866 (1989).

³O. Hildebrand, W. Kuebart, and M. H. Pilkuhn, Appl. Phys. Lett. **37**, 801 (1980).

⁴S.-M. Kim, S.-H. Lee, J.-K. Shin, J.-Y. Leem, J.-S. Kim, and J.-S. Kim, J. Korean Phys. Soc. **40**, 119 (2002).

⁵M. E. Twigg, B. R. Benett, P. M. Thibado, B. V. Shanabrook, and L. J. Whitman, Philos. Mag. A **7**, 7 (1998).

⁶W. E. Hoke, T. D. Kennedy, A. Torabi, C. S. Whelan, P. F. Marsh, R. E. Leoni, C. Xu, and K. C. Hsieh, J. Cryst. Growth **251**, 827 (2003).

⁷W. E. Hoke, P. J. Lemonias, T. D. Kennedy, A. Torabi, E. K. Tong, K. L. Chang, and K. C. Hsieh, J. Vac. Sci. Technol. B **19**, 1519 (2001).

⁸T. S. Zheleva, O.-H. Nam, W. M. Ashmawi, J. D. Griffin, and R. F. Davis, J. Cryst. Growth **222**, 706 (2001).

⁹M. Hansen, P. Fini, M. Craven, B. Heying, J. S. Speck, and S. P. DenBaars, J. Cryst. Growth **234**, 623 (2002).

¹⁰A. A. Khandekar, G. Suryanarayanan, S. E. Babcock, and T. F. Kuech (unpublished).

¹¹P. Hazdra, J. Voves, J. Oswald, E. Hulcius, J. Pangrac, and T. Simecek, J. Cryst. Growth **248**, 328 (2003).

¹²G. Suryanarayanan, A. A. Khandekar, T. F. Kuech, and S. E. Babcock, Mater. Res. Soc. Symp. Proc. **744**, 9 (2002).